

## Visible channel development during the initial breakdown of a natural negative cloud-to-ground flash

Leandro Z. S. Campos<sup>1</sup> and Marcelo M. F. Saba<sup>1</sup>

Received 10 July 2013; revised 19 August 2013; accepted 22 August 2013; published 10 September 2013.

[1] GPS time synchronized high-speed video records (at 4000 frames per second) and electric field waveforms are discussed for one stepped leader of a negative cloud-to-ground flash whose initial development becomes visible above cloud base. The leader emerges from the opaque region of the thundercloud around 4800 m above ground, propagating with speeds of the order of  $10^6$  m s<sup>-1</sup>. It is possible to see that this early, bright, and fast propagation period occurred simultaneously with the emission of initial breakdown bipolar pulse trains. The leader gradually reduces its speed and luminous intensity: When its tip is less than 3000 m above the ground, the propagation speeds oscillate between 2 and  $4 \times 10^5$  m s<sup>-1</sup> until it makes contact approximately 16 ms after it first became visible. With time, the initial breakdown waveform is gradually replaced by unipolar pulses and the leader propagation speed drops to the  $10^5$  m s<sup>-1</sup> range. **Citation:** Campos, L. Z. S., and M. M. F. Saba (2013), Visible channel development during the initial breakdown of a natural negative cloud-to-ground flash, *Geophys. Res. Lett.*, *40*, 4756–4761, doi:10.1002/grl.50904.

### 1. Introduction

[2] The single-station electric field study of *Clarence and Malan* [1957] identified that the waveform that precedes the first negative stroke can be divided into three different parts: breakdown (B), intermediate stage (I), and stepped leader development (L). They suggested that the breakdown pulses are associated with an electrical discharge between charge centers inside the thundercloud, comprising a phenomenon that is distinct from the stepped leader itself. Further electric field analyses addressed the characteristics of the initial breakdown (IB) pulse train in the early development of both ground and cloud flashes [e.g., *Weidman and Krider*, 1979; *Beasley et al.*, 1982; *Nag et al.*, 2009], showing that their waveform are of bipolar nature with pulse widths of tens of microseconds.

[3] Through the analysis of lightning VHF radio emissions, *Proctor et al.* [1988] were able to correlate the IB pulse activity with the start of the stepped leader propagation. More recently, *Nag and Rakov* [2009] evaluated qualitatively the effect of lower positive charge region (LPCR) of a thundercloud over what type of lightning it will produce based on the breakdown pulse train. They suggest that the IB pulse

trains are emitted during the propagation of a negative leader through the LPCR. In such context, one would expect that ground flashes produced in a cloud with a large LPCR present an IB pulse train in its early development, but a cloud with a small LPCR would produce ground flashes with no IB pulse activity [*Nag and Rakov*, 2009, section 2.3 and Figure 3].

[4] New insights on the phenomenology of lightning breakdown processes were given by *Stolzenburg et al.* [2013], who studied bursts of light during the emission of the IB pulses. In some of the events they analyzed, there were linear segments propagating away from the initial light emission in an intermittent fashion, decreasing its luminosity between subsequent bursts that progressively extends its path. The intermittency of this early leader or streamer could be resolved due to the high frame rate of the high-speed camera used in their study (either 50,000 or 54,000 frames per second).

[5] Balloon soundings showed that the electric fields measured inside thunderclouds are too low for the conventional breakdown mechanism. For that reason, alternative mechanisms have been proposed. For example, *Gurevich et al.* [2004] suggested that a combination runaway breakdown (a mechanism in which the number of relativistic and thermal electrons in air rapidly increases through an avalanche-like process) and extensive atmospheric showers (cascades of secondary ionized particles and electromagnetic radiation produced by the interaction of primary cosmic rays with air molecules in the atmosphere) might be responsible for the initiation of leader development in lightning. *Gurevich and Karashtin* [2013] further developed that idea by considering that the runaway breakdown/extensive atmospheric shower mechanism is enhanced when it occurs in the presence of electrically charged hydrometeors and suggested that this process occurs between the main negative charge region and the LPCR of the thundercloud. In this wide context, one may argue that the study of IB processes have relevant implications for the knowledge not only of lightning as a phenomenon but also of the atmospheric, meteorological, and cosmic context where it occurs.

[6] The present work consists in the analysis of one negative cloud-to-ground flash whose first return stroke was initiated by a leader that left the thundercloud optically opaque region before crossing the cloud base. Clear channel development and branching could be seen to occur simultaneously with the IB pulse trains. This observational fact can be of importance for the current knowledge of the physics of lightning initiation.

### 2. Instrumentation

[7] The event analyzed in the present work was observed with the help of a high-speed digital camera, three electric

<sup>1</sup>ELAT/CCST, National Institute for Space Research, São José dos Campos, São Paulo, Brazil.

Corresponding author: L. Z. S. Campos, ELAT/CCST, National Institute for Space Research, Av. dos Astronautas, 1758, CEP 12227-010, São José dos Campos, SP, Brazil. (leandro.zanella@gmail.com)

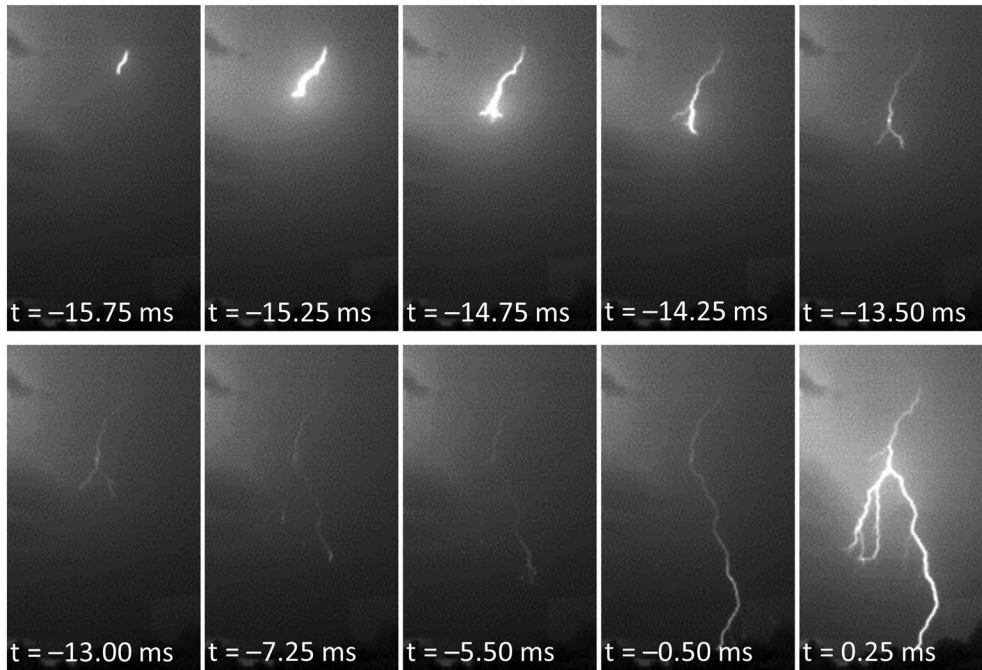


**Figure 1.** Selection of sectioned frames of the high-speed camera record of the analyzed leader. The last frame corresponds to the visible channel shape 250  $\mu$ s after the return stroke.

field sensors (two fast antennas with different gains and one slow antenna), and data from a lightning locations system. They were all operated during the summer of 2010/2011 in São José dos Campos, São Paulo, Brazil. Details on each instrument are provided in the following subsections.

### 2.1. High-Speed Camera

[8] A Photron FASTCAM 512 PCI was operated during the 2010/2011 summer at temporal resolution of 4000 frames per second (approximately 250  $\mu$ s of exposure time). Each frame had a spatial resolution of 512 (horizontal) per 256 (vertical) pixels and each pixel had an 8 bit pixel depth (256 levels of grey). Global Positioning System (GPS) time synchronization was made possible with the help of a dedicated antenna, allowing a detailed comparison of the time-stamped images with data provided by other instruments. With the help of a detailed comparison between video data provided by the camera and fast electric field data, it was possible to conclude that the time stamping is done at the beginning of the exposure of each frame. Finally, the manufacturer informs that there is no frame-to-frame persistency, which allows a clear analysis of the leader progression.

[9] The system was operated manually, triggered with the help of a button pressed at the moment that the operator sees one return stroke. It was set to record 1 s prior to and 1 s after the triggering moment. Such configuration is usually adequate to allow the whole flash, considering both the reaction time of the operator and the total flash duration of both polarities [e.g., *Saraiva et al.*, 2010, Figures 6 and 7; *Saba et al.*, 2010, Figure 8].

### 2.2. Electric Field Sensors

[10] Three different electric field sensors were operated simultaneously. They consisted of flat plate antennas with an integrator/amplifier circuit (with a bandwidth that ranged from 306 Hz to 1.5 MHz), GPS system for time synchronization,

and a digital data acquisition system (with a 12 bit analog/digital converter sampling at a rate of 5 MS/s). Two of the sensors were operated as fast antennas (resistance-capacitance decay time constant of approximately 500  $\mu$ s) with sensitivities different by a factor of 10. The third used a distinct circuit designed to behave as a slow electric field change sensor (with a decay constant of 1.5 s).

### 2.3. Brazilian Lightning Location Network (BrasilDAT)

[11] Data provided by the Brazilian Lightning Location Network (BrasilDAT) were used to estimate the distance between the instruments and the ground strike point of the analyzed event. Such information is vital for the channel length and speed estimates presented, as discussed in the following section. The region of interest for the present study is well covered by the BrasilDAT at the time of the data collection [*Naccarato and Pinto*, 2009].

## 3. Observation Analysis

[12] The event of interest for the present work is the leader that preceded the first stroke of a three-stroke flash that occurred on 2 February 2011, at 18:01:45 universal time (UT) in São José dos Campos, São Paulo, Brazil. The interstroke intervals between the first stroke (discussed in detail here) and the second, and between the second and the third strokes, were 24.50 and 33.75 ms, respectively. The second and third strokes diverged partially from the channel originally created by the first channel but touched ground at the same strike point. Only the third stroke was detected by the BrasilDAT but, as it had the same ground contact point as the first stroke, its location estimate (14.6 km away from the instruments) was used for the photogrammetric analysis of channel length and leader speed presented in this section. Considering the camera and lens configuration, each pixel was estimated to cover a square area of approximately 40 by 40 m on a plane

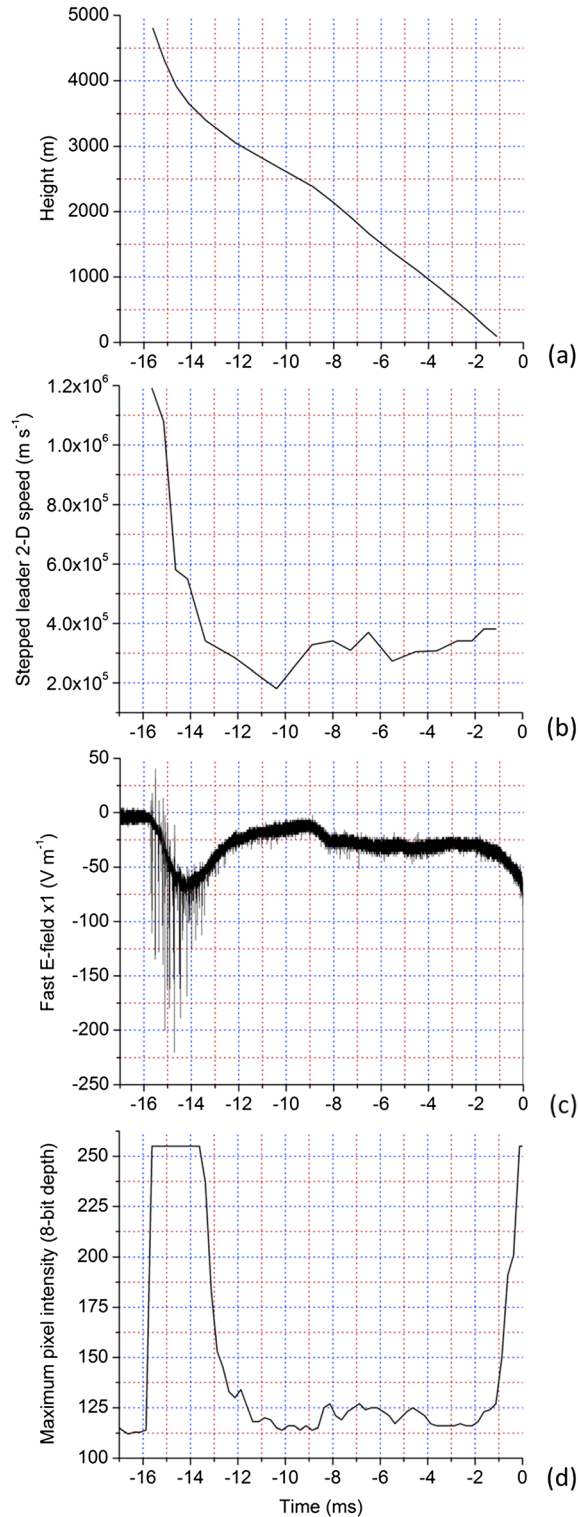


**Figure 2.** Temporal evolution of the analyzed event in terms of (a) leader tip height, (b) 2-D leader speed, (c) fast electric field change (following the physics sign convention), and (d) maximum pixel intensity value per frame. Time  $t=0$  corresponds to the moment of return stroke occurrence, and the decay time constant of the fast electric field sensor is approximately 500  $\mu\text{s}$ .

parallel to the charge-coupled device (CCD) sensor (and located 14.6 km away from it). The BrasilDAT reported an estimated peak current for the third stroke of  $-12$  kA. By assuming a linear relationship between return stroke current and electric field peak values and considering that all three strokes had the same ground strike point, it was possible to estimate from the fast electric field records that the first and second strokes had peak currents of  $-35$  and  $-36$  kA, respectively.

[13] Taking time  $t=0$  at the moment of occurrence of the first return stroke, 18:01:45.859250s (UT), at  $t=-16.00$  ms, a very faint channel segment became visible, leaving the opaque region of the cloud above its base (approximately 4800 m from the ground). For the sake of comparison, the negative charge region of warm season thunderstorms in the region where the observation was made is usually located close to 6500 m above ground [e.g., *Saraiva et al.*, 2010, section 2]. In the following video frame, time stamped at  $t=-15.75$  ms, the channel luminosity became much more intense, making it possible to see the channel formation as the leader progressed toward ground (as shown in the selected frames presented in Figure 1). At this early stage, the two-dimensional (2-D) leader speed was of the order of  $10^6$  m s<sup>-1</sup>, considerably high when compared to the typical values associated with stepped leaders [e.g., *Schonland*, 1938, section 3 ; *Berger and Vogelsanger*, 1966, Table 1; *Campos et al.*, 2013, Figure 2]. During the following 2 or 3 ms, the development speed drops to more commonly reported speeds of the order of  $10^5$  m s<sup>-1</sup> roughly at the same time as its emitted luminosity becomes progressively lower (as shown in the upper line of frames of Figure 1). It is worth noting that the channel developed some branching during this early development, as shown in the frames at  $t=-14.75$  and  $t=-14.25$  ms of Figure 1.

[14] Another important characteristic of the early phase of the development of this event can be seen on the graphs of Figure 2. It presents the temporal evolution of (a) leader tip height, (b) 2-D leader speed, (c) fast electric field change (provided by the antenna with the lower gain) following the physics sign convention, and (d) maximum pixel intensity value per frame. As the leader progresses continuously, Figure 2d was obtained with the help of a modified version of the algorithm used by *Campos et al.* [2007, 2009] for their studies on M component parameters. Instead of averaging the pixel values over a fixed area, the modified algorithm obtains the maximum luminosity value over the entire frame, making it possible to determine the intensity of the core of the channel. Through the analysis of Figure 2, it is possible to notice that the leader becomes visible almost simultaneously with the emission of the intense initial breakdown pulses (IB) that can be observed by the fast electric field antenna (around  $t=-15.75$  ms). The fast and bright period of leader propagation is not only accompanied by the IB pulses but also by a slowly varying “hump-like” (roughly 4 ms long) electric field change, over which the pulses are superimposed. The pulse activity presents peak values progressively lower as the channel brightness decreases along with the leader tip, whose speed drops to values below  $6 \times 10^5$  m s<sup>-1</sup> at heights close to 3500 m. From that point until the leader touches ground and produces the return stroke, its 2-D speed oscillates between  $2 \times 10^5$  and  $4 \times 10^5$  m s<sup>-1</sup>, never reaching again the high values of its early development. A comparison between Figures 2b and 2c also shows that the initial, faster propagation of the leader coincides with the electric field “hump” over which the IB pulse activity is superimposed. Similar

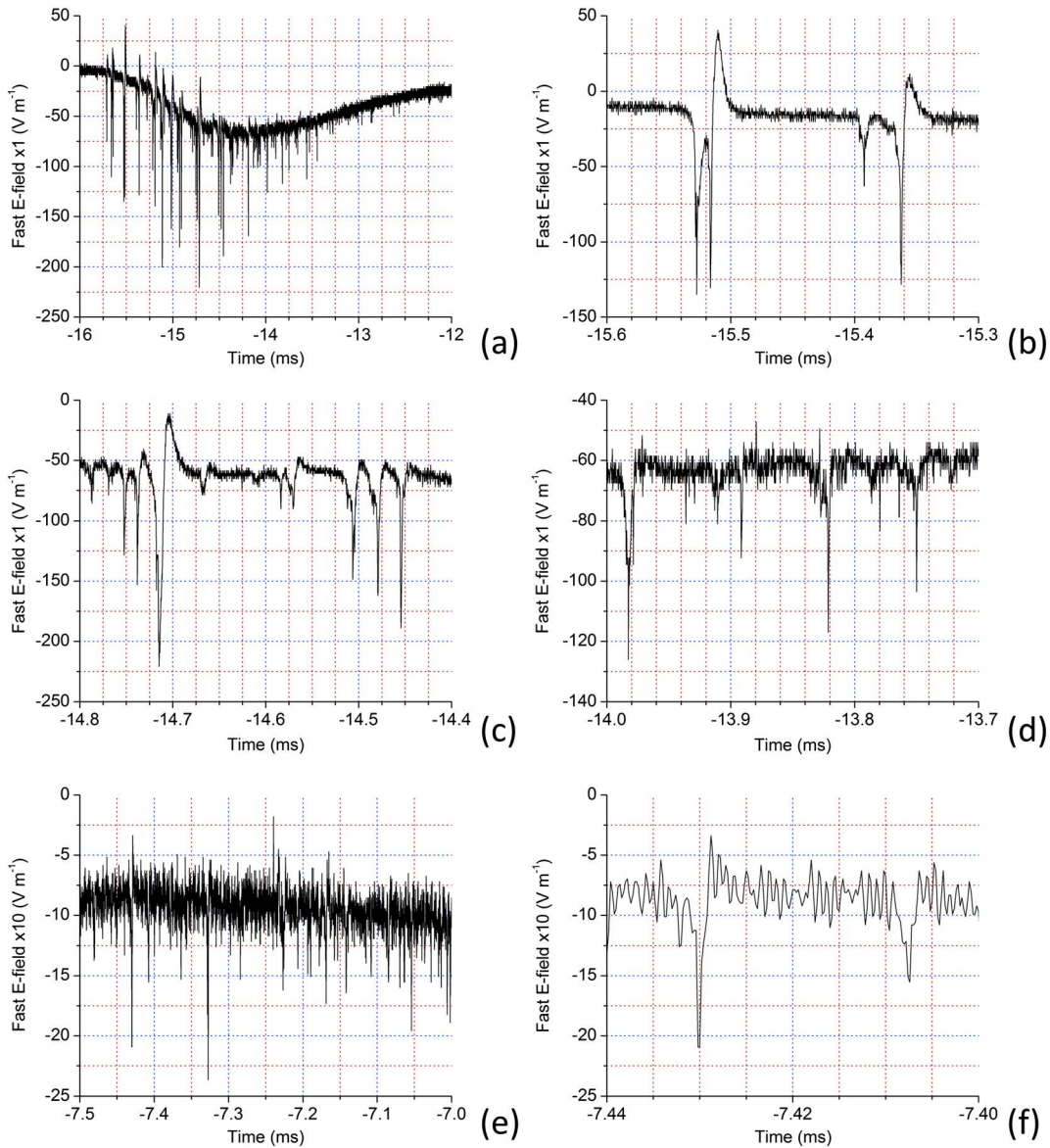


**Figure 3.** Fast electric field waveforms of each phase of the analyzed event: (a) slowly varying “hump” change over which the initial breakdown pulses are superimposed, (b) two initial breakdown pulse trains, (c) and (d) transition between bipolar and mostly unipolar pulses, (e) lower intensity (close to noise level) pulses emitted during the less luminous part of leader propagation, and (f) individual pulses of the late leader development, shown in Figure 3e. All the waveforms follow the physics sign convention, time  $t=0$  corresponds to the moment of return stroke occurrence, and the decay time constant of the fast electric field sensor is approximately 500  $\mu\text{s}$ .

slowly varying field changes were also observed to precede the two subsequent strokes; on their cases, however, it was not possible to notice similar superimposed IB pulses. Given the limited temporal resolution of the camera (4000 frames per second), it was not possible to resolve individual stepping of the leader progression during any period. The slow electric field waveform, not included in Figure 2, showed only a steady intensification as the leader gets closer to ground. Also, it is important to acknowledge two relevant limitations of the available data for this event: (i) it is not possible to determine if the channel started developing before leaving the cloud opaque region, and (ii) it is possible that either most or all the observed IB pulse activity was produced by another branch that remained hidden inside the thundercloud.

[15] Figure 3 shows details of the fast electric field waveforms of different phases of the leader development. In Figure 3a, it is possible to see the slowly varying hump over which the IB pulses are superimposed and how their amplitude decreases progressively with time after the hump minimum. Two of the IB pulses superimposed on the first part of the hump are shown in detail in Figure 3b. The bipolar nature of these pulses is easily noticeable: two negative pulses followed by a positive deflection (physics sign convention). Similarly to what was reported by *Stolzenburg et al.* [2013], the observed pulses would fit into the “classical” definition presented by *Nag et al.* [2009, Figure 2] and resembles those reported by previous researchers, such as *Weidman and Krider* [1979, Figure 4] for intracloud discharges. As

commented by *Rakov and Uman* [2003, p. 119], the amplitude of the IB pulses can be comparable to those of the following return strokes. For the analyzed event, for instance, the ratio between the return stroke and the largest IB pulse (which occurred at  $t = -14.72$  ms) was approximately 1.9.

[16] As time advances, the overall waveform of the electric field pulses change. The positive deflection becomes progressively lower (Figure 3c), to the point in which the pulses appear to be essentially unipolar (Figure 3d). This transition seems to be associated with the decrease in the leader luminous intensity, as indicated through a comparison between the fast electric field hump decay (Figure 2c) and the moment that the maximum pixel value per frame drops below saturation level (Figure 2d). This transition is also evident in Figure 1 if one compares the channel intensity of the frame recorded at  $t = -14.25$  ms with the frame recorded at  $t = -13.00$  ms.

[17] The final and slower phase of the leader propagation the electric field pulse activity seems to correspond to the typical stepped leader waveform. Figures 3e and 3f show such pulses, whose amplitudes are close to the system noise level and that are separated typically by a few tens of microseconds. Differently from the other electric field waveforms presented in this paper, for these pulses it was necessary to use the data provided by the fast antenna with the highest gain in order to differentiate it from the noise level.

#### 4. Discussion

[18] The analysis of the high-speed video and fast electric field data of the leader event indicated that the IB pulse trains occur simultaneously with the development of the lightning channel. It is not clear whether or not this early phase consists of a streamer (transient air discharge with a filamentary structure, low temperatures, and currents of low intensity) or a leader (a hot, high-current process capable of ionizing kilometer-long plasma channels). Laboratory long spark experiments have shown that leaders are initiated by a number of streamer discharges [*Gallimberti et al.*, 2002]; however, considering the very intense luminous emission reported here, the authors expect that the observed channel development is produced by a leader.

[19] The phenomenology observed in the analyzed event is similar to the very recent reports presented by *Stolzenburg et al.* [2013]. Due to the limited frame rate of our camera (4000 frames per second) compared to the one they used (either 50,000 or 54,000 frames per second), it was not possible to resolve the linear features of the early channel development that occurs simultaneously with the IB pulse trains. It is mentioned in their work's abstract that the "linear segments visibly advance away from the first light burst for 55–200  $\mu\text{s}$ ", so if the reported intermittency occurred in the event analyzed in the present work, it was probably undetectable due to the relatively long exposure time of the used camera (roughly 250  $\mu\text{s}$ ).

[20] The 2-D speeds of the analyzed event during its early development (initially  $1.2 \times 10^6$  m s<sup>-1</sup> then dropping progressively to roughly  $3 \times 10^5$  m s<sup>-1</sup> after 3 ms) lies within the range estimated by *Stolzenburg et al.* [2013, p. 18], which was "about 4–18  $\times 10^5$  m s<sup>-1</sup> over the first few hundred microseconds and decrease by about 50% over the first 2 ms." Also, the early, faster development phase coincided with a slowly varying hump-like electric field change over which

the IB pulses were superimposed. One important difference between the case analyzed here and those discussed by *Stolzenburg et al.* [2013] is the fact that no nonluminous period was observed after the last large IB pulse. Considering the typical durations of such period that were reported (between 1 and 2 ms [*Stolzenburg et al.*, 2013, p. 19]), it would have been observed at the available temporal resolution (250  $\mu\text{s}$ ). However, the high-speed camera data, which is reproduced partially in Figure 1, showed no cessation of channel luminosity. What can be argued is that, as the channel brightness suffers a progressive reduction after the early fast propagating phase, the intervening cloud between their camera and the developing channel caused the apparent luminosity cessation reported by *Stolzenburg et al.* [2013].

[21] In order to compare our observations with the qualitative inferences presented by *Nag and Rakov* [2009] on the effect of the LPCR over the leader propagation, sounding data were obtained. The chosen station is located at the Campo de Marte Airport, approximately 105 km away from the ground contact point estimated by BrasilDAT. Soundings obtained roughly 6 h prior to and after the flash of interest were available (i.e., at 12:00 UT of the same day and 00:00 UT of the next day, respectively). Considering that the sounding data are a good approximation for the profile at the flash occurrence region and period, the negative charge center (corresponding to the range of heights between the temperatures  $-10^\circ\text{C}$  and  $-25^\circ\text{C}$ ) is expected to be located roughly between 6500 and 9400 m above ground level. With the photogrammetric analysis of the leader, one might say that the flash initiation point was roughly 2 km below the negative charge center. At the same time, assuming that the LPCR is located just below freezing level, it should be found between 4300 and 4900 m above ground. That corresponds to the range of heights where the leader starts its visible development toward ground: its early, fast ( $1.2 \times 10^6$  m s<sup>-1</sup> then dropping progressively to  $5.8 \times 10^5$  m s<sup>-1</sup>) and bright development phase takes place between 4800 and 3900 m above ground (Figure 2). Assuming that the freezing level indeed corresponds to the LPCR, the assumption introduced by *Nag and Rakov* [2009] that the IB pulse trains are emitted as the stepped leader progresses through the LPCR seems plausible under the light of the analysis of the present paper. However, it is important to stress the fact that it was not possible to determine whether or not there was channel development taking place before the leader left the opaque region of the thundercloud and started to emit the IB pulses while entering the range of heights of the LPCR, as *Nag and Rakov* [2009, section 2.1] suggested. Additionally, it is necessary to acknowledge the possibility that most of the IB pulse activity could be produced by another branch, hidden inside the opaque region of the thundercloud.

[22] *Schonland* [1938, section 9] identified two types of stepped leader. Type  $\alpha$ , the most common, "moves in a fairly regular manner from cloud to ground without excessive branching." Type  $\beta$ , on the other hand, was said to be less common (30% of his analyzed cases) and "much faster and brighter in its initial stages than the  $\alpha$  type", presenting speed of the order of  $10^6$  m s<sup>-1</sup>. *Schonland* [1938] also mentions that  $\beta$  type leaders are usually highly branched in their upper regions, near cloud base. Based on that description, the data suggest that the event analyzed in the present work would have been classified as a type  $\beta$  leader if one considers the historical terminology, with the exception of the early

prominent branching (which was not particularly extensive, as seen on Figure 1). However, as suggested by *Beasley et al.* [1982] based on electric field records,  $\alpha$  and  $\beta$  leaders do not seem to be distinct phenomena. If only the later phase (below 2 km) of the leader development could be observed, it would have been seen as a regular  $\alpha$  leader.

[23] Finally, it is worth mentioning that, similarly to the study of *Stolzenburg et al.* [2013, p. 19], even though the analysis is completely focused on the development of a negative downward leader, no information is available to confirm or deny the existence of an upward-moving positive end of the early fast development.

## 5. Concluding Remarks

[24] The analysis of the channel development of the first stroke of a negative cloud-to-ground flash that leaves the opaque region of the thundercloud above cloud base was presented in detail. The available data suggest that the beginning of the initial breakdown pulse trains coincide with an early, fast ( $10^6 \text{ m s}^{-1}$ ), and bright leader or streamer propagation. As time advanced, the waveform of the observed pulses changed from the bipolar structure of initial breakdown to a unipolar one. This transition coincides with the reduction of the channel luminosity and propagation speed (which drops to  $10^5 \text{ m s}^{-1}$ ). The final phase of the channel formation presents itself as a regular stepped leader, making ground contact roughly 16 ms after it became first visible.

[25] A comparison between the analyzed event and those reported by *Stolzenburg et al.* [2013] suggested that both works report the same type of phenomenon. Some differences that were discussed may be attributed to the differences in visibility and camera frame rates. A brief evaluation of *Nag and Rakov* [2009] hypothesis on the production of the initial breakdown pulses (which they suggest to be related to the interaction between the stepped leader and the lower positive charge region) was presented. It was concluded that their interpretation is indeed possible based on some minor assumptions. It is also speculated that the type  $\beta$  leaders, introduced by *Schonland* [1938], may actually consist of regular stepped leaders that become visible during its early, faster development phase.

[26] Many discussions are being conducted on the role of cosmic rays and high-energy processes in the early phases of lightning development, so it is also expected that the observations reported in the present work might shed additional light on that problem. The fact that there was visible channel development simultaneously with the IB pulse activity and the reported range of heights at which these processes occurred may be relevant to researchers dedicated to the study of runaway breakdown initiating lightning.

[27] **Acknowledgments.** The authors are grateful to C. Schumann, C. Medeiros, R. da Silva, S. Viegas, and C. Lopes for their assistance in data collection and reduction, and to W. Schulz for providing the schematics and software used for the electric field sensor and data acquisition system. This research

has been supported by CNPq and FAPESP through the projects 475299/2003-5 and 03/08655-4, respectively. One of the authors (L.Z.S.C.) is also grateful to FAPESP for the scholarship 2010/02716-5.

[28] The Editor thanks two anonymous reviewers for their assistance evaluating this manuscript.

## References

- Beasley, W., M. A. Uman, and P. L. Rustan Jr. (1982), Electric fields preceding cloud-to-ground lightning flashes, *J. Geophys. Res.*, *87*, 4883–4902.
- Berger, K., and E. Vogelsanger (1966), Photographische blitzuntersuchungen der jahre 1955–1965 auf dem Monte San Salvatore, *Bull. Schweiz. Elektrotech. Ver.*, *57*, 599–620.
- Campos, L. Z. S., M. M. F. Saba, O. Pinto Jr., and M. G. Ballarotti (2007), Waveshapes of continuing currents and properties of M-components in natural negative cloud-to-ground lightning from high-speed video observations, *Atmos. Res.*, *84*, 302–310, doi:10.1016/j.atmosres.2006.09.002.
- Campos, L. Z. S., M. M. F. Saba, O. Pinto Jr., and M. G. Ballarotti (2009), Waveshapes of continuing currents and properties of M-components in natural positive cloud-to-ground lightning, *Atmos. Res.*, *91*, 416–424, doi:10.1016/j.atmosres.2008.02.020.
- Campos, L. Z. S., M. M. F. Saba, T. A. Warner, O. Pinto Jr., E. P. Krider, and R. E. Orville (2013), High-speed video observations of natural cloud-to-ground lightning leaders – a statistical analysis, *Atmos. Res.*, doi:10.1016/j.atmosres.2012.12.011.
- Clarence, N. D., and D. J. Malan (1957), Preliminary discharge processes in lightning flashes to ground, *Q. J. R. Meteorol. Soc.*, *83*, 161–172.
- Gallimberti, I., G. Bacchiega, A. Bondiou-Clergerie, and P. Lalande (2002), Fundamental processes in long air gap discharges, *C. R. Physique*, *3*, 1335–1359, doi:10.1016/S1631-0705(02)01414-7.
- Gurevich, A. V., and A. N. Karashtin (2013), Runaway breakdown and hydrometeors in lightning initiation, *Phys. Rev. Lett.*, *110*, 185005, doi:10.1103/PhysRevLett.110.185005.
- Gurevich, A. V., Y. V. Medvedev, and K. P. Zybin (2004), New type discharge generated in thunderclouds by joint action of runaway breakdown and extensive atmospheric shower, *Phys. Lett. A*, *319*, 348–263, doi:10.1016/j.physleta.2004.06.099.
- Naccarato, K. P., and O. Pinto Jr. (2009), Improvements in the detection efficiency model for the Brazilian lightning detection network (BrasilDAT), *Atmos. Res.*, *91*, 546–563, doi:10.1016/j.atmosres.2008.06.019.
- Nag, A., and V. A. Rakov (2009), Some inferences on the role of lower positive charge region in facilitating different types of lightning, *Geophys. Res. Lett.*, *36*, L05815, doi:10.1029/2008GL036783.
- Nag, A., B. A. DeCarlo, and V. A. Rakov (2009), Analysis of microsecond- and submicrosecond-scale electric field pulses produced by cloud and ground lightning discharges, *Atmos. Res.*, *91*, 316–325, doi:10.1016/j.atmosres.2008.01.014.
- Proctor, D. E., R. Uytendogaardt, and B. M. Meredith (1988), VHF radio pictures of lightning flashes to ground, *J. Geophys. Res.*, *93*, 12,683–12,727.
- Rakov, V. A., and M. A. Uman (2003), *Lightning: Physics and Effects*, pp. 687, Cambridge Univ. Press, New York.
- Saba, M. M. F., W. Schulz, T. A. Warner, L. Z. S. Campos, C. Schumann, E. P. Krider, K. L. Cummins, and R. E. Orville (2010), High-speed video observations of positive lightning flashes to ground, *J. Geophys. Res.*, *115*, D24201, doi:10.1029/2010JD014330.
- Saraiva, A. C. V., M. M. F. Saba, O. Pinto Jr., K. L. Cummins, E. P. Krider, and L. Z. S. Campos (2010), A comparative study of negative cloud-to-ground lightning characteristics in São Paulo (Brazil) and Arizona (United States) based on high-speed video observations, *J. Geophys. Res.*, *115*, D11102, doi:10.1029/2009JD012604.
- Schonland, B. F. J. (1938), Progressive lightning. IV. The discharge mechanism, *Proc. R. Soc. Lond.*, *A164*, 132–150.
- Stolzenburg, M., T. C. Marshall, S. Karunarathne, N. Karunarathna, L. E. Vickers, T. A. Warner, R. E. Orville, and H.-D. Betz (2013), Luminosity of initial breakdown in lightning, *J. Geophys. Res. Atmos.*, *118*, 2918–2937, doi:10.1002/jgrd.50276.
- Weidman, C. D., and E. P. Krider (1979), The radiation field wave forms produced by intracloud lightning discharge processes, *J. Geophys. Res.*, *84*, 3159–3164.